SYNTHESIS AND CHARACTERIZATIONS OF PURE AND DOPED NANOCRYSTALLINE $BiFeO_3$ CERAMICS BY SHS

#YOGESH A. CHAUDHARI*, CHANDRASHEKHAR M. MAHAJAN**, SUBHASH T. BENDRE***

** Department of Physics, Shri. Pancham Khemraj Mahavidyalaya, Sawantwadi-416 510 (M.S.)*
(Affiliated to Mumbai University) India
***Department of Engineering Sciences and Humanities (DESH),*
Vishwakarma Institute of Technology (VIT), Pune – 410 405 (M.S) India
****Department of Physics, School of Physical Sciences,*
North Maharashtra University, Jalgaon - 425 001 (M.S) India

#E-mail: parthsindhu@gmail.com

Submitted June 26, 2013; accepted March 8, 2014

Keywords: $BiFeO_3$ Ceramics, SHS, XRD, Ferroelectrics, Multiferroics, Dielectrics

The pure and Zn incorporated $BiFeO_3$ ceramics were synthesized by self-propagating high temperature synthesis (SHS). The X-ray diffractometer (XRD) studies revealed that, both $BiFeO_3$ and $BiFe_{0.95}Zn_{0.05}O_3$ ceramics crystallizes in a single phase rhombhohedral structure. The room temperature ferroelectric and magnetic hysteresis loop evidenced coexistence of ferroelectricity and magnetism in single phase undoped and Zn doped $BiFeO_3$. The M-H hysteresis loop of $BiFe_{0.95}Zn_{0.05}O_3$ sample demonstrated a weak ferromagnetism at 300 K and 5 K respectively. The room temperature ferroelectric P-E hysteresis loops of $BiFeO_3$ and $BiFe_{0.95}Zn_{0.05}O_3$ exhibited an unsaturated behavior and suggests a partial reversal of polarization. A variation of dielectric constant with respect to temperature in $BiFeO_3$ and $BiFe_{0.95}Zn_{0.05}O_3$ ceramic delivers a dielectric anomaly around 480 and 450°C which is a consequence of antiferromagnetic to paramagnetic phase transition (TN). Moreover, for $BiFeO_3$ the anomaly manifests a possible coupling between electric and magnetic dipole moments.

INTRODUCTION

Multiferroic material exhibits an electric and magnetic nature collectively, which results in mutual existence of ferroelectricity and ferromagnetism in a single phase [1]. Furthermore the coupling between electric and magnetic ordered parameters, brings forth an unique phenomena known as magnetoelectric effect (ME). In ME effect the magnetization can be switched by enforcing electric field and polarization can be switched by applying magnetic field. This offers an additional opportunity for designing microelectronic, spintronic devices [2-4]. The multiferroic materials have acquired a great deal of interest due to their potential applications in several fields such as information storage, spintronic sensors [5], thin film capacitor, nonvolatile memory, nonlinear optics, photoelectrochemical cell, magnetoelectric sensor devices, multiple state memories, high density ferroelectric random access memory, electric field controlled ferromagnetic resonance devices, radio-transmission, microwave, satellite communication, digital recording and permanent magnet applications [6-10]. The multifunctional $BiFeO_3$ shows extremely interesting characteristics due to its higher ferroelectric Curie temperature T_c ~ 1103 K and G-type antiferromagnetic Neel temperature T_N ~ 643 K [11, 12].

Recently, several co-workers have made an attempt towards the improvement of multiferroic properties in $BiFeO_3$ using different trivalent dopants such as Nd [13], La [14], Cr [15], Ti [16], Sm [17] and Mn [5]. In this concern, there have been few reports on the ferroelectric and dielectric properties of $BiFeO_3$ using divalent dopants such as, Kothari et al. reported the multiferroic properties of $Bi_{1-x}Ca_xFeO_3$ system by solid state reaction and proved that the leakage current increases with varying Ca doping [18]. The ferroelectric and dielectric property of solid state synthesized $Bi_{1-x}Ba_xFeO_3$ compound proves unsaturated ferroelectric hystersis loops with existence of magnetoelectric coupling in the compound by Wang et al. [19]. The ferroelectric properties of $Bi_{1-x}Ba_xFeO_3$ compound by Gautam et al. have shown lower resistivity in higher leakage current range, however, the dielectric constant and loss decreases with increasing frequency [20]. Recently Xu et al. studied the significantly improved dielectric properties of Zn doped $BiFeO_3$ ceramics formulated by rapid sintering method [21].

In this amazement, the present paper reports the synthesis of pure as well as Zn doped $BiFeO_3$ ceramics by self propagating high temperature synthesis (SHS) and describes their ferroelectric, magnetic and dielectric properties.

EXPERIMENTAL

Materials

The $Bi(NO_3)_3.5H_2O$ (CDH, India), $Fe(NO_3)_3.9H_2O$ (Fischer Scientific), $Zn(NO_3)_2.6H_2O$ (CDH, India) were used as a starting precursor and glycine (NH_2CH_2COOH) (CDH, India) was used as a fuel for the synthesis of $BiFeO_3$ and $BiFe_{0.95}Zn_{0.05}O_3$ ceramics. The metal nitrates were used as oxidizers whereas glycine played the role of fuel for the combustion reaction.

Synthesis process of compounds

The $BiFeO_3$ and $BiFe_{0.95}Zn_{0.05}O_3$ ceramics were prepared by self propagating high temperature synthesis (SHS). For this, the oxidizers (O): fuel (F) ratio was calculated on the basis of oxidizing valencies of metal nitrates and reducing valency of fuel [22-24]. The above mentioned metal nitrates and glycine in stochiometric ratios were dissolved in distilled water. Afterwards, the mixture was heated in Pyrex dish (150 × 50 mm^2) on a burner until the excess of free water evaporates and at the same time spontaneous ignition occurred; thereafter, a combustion powders were obtained. These powders of $BiFeO_3$ and $BiFe_{0.95}Zn_{0.05}O_3$ were grinded and calcined for phase formation of ceramics. In addition, these powders were pelletized through addition of polyvinyl alcohol (PVA) as binder. Lastly, these pellets were sintered at higher temperatures as 625°C and 650°C for 15 min. Finally, these pellets were carried out for further experimental work. The previous flowchart summarizes the complete methodology for the preparation of materials.

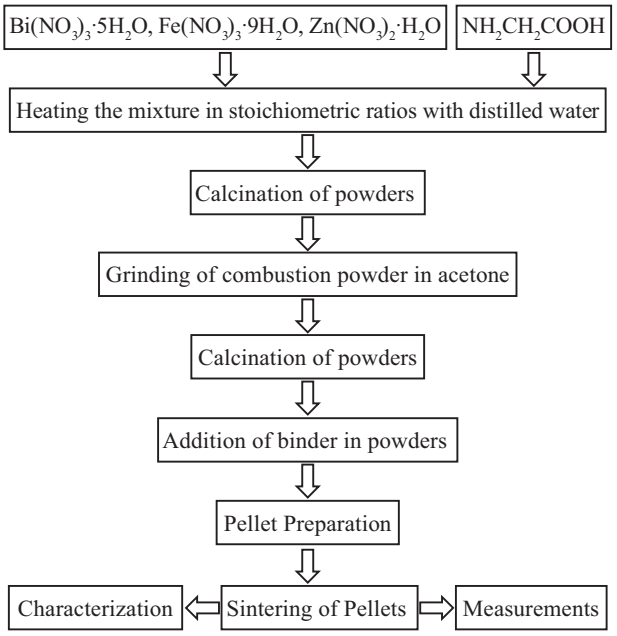

Characterizations

The structural analysis and phase identification of the sintered pellet was performed on X-ray diffractometer (Philips X'Pert PRO) with CuKα radiation in the 2θ range 20 - 70°. The surface morphology of samples was studied by using scanning electron microscope (SEM, EVO-50). The suitable ohmic contacts were prepared with conducting silver paint (RS Components - UK) for ferroelectric and dielectric measurements the two opposite surfaces of sintered pellets were polished with silver paste. Ferroelectric measurements were performed at room temperature using Precision Premier II, Radiant Technologies, USA. Dielectric constant measurement as a function of temperature measurement of the samples in the temperature range 30 - 500°C at certain fixed frequencies 1 kHz, 3 kHz and 5 kHz were carried out using Agilent HP 4192A, Impedance Analyzer.

RESULTS AND DISCUSSION

Structural Studies

The room temperature (RT) X-ray diffraction patterns of $BiFeO_3$ and $BiFe_{0.95}Zn_{0.05}O_3$ samples are as shown in Figure 1. The XRD pattern reveals that, both the ceramic sample crystallizes in a rhombhohedral perovskite phase. An additional impurity phase were observed around 30° corresponds to $Bi_{12}(Bi_{0.5}Fe_{0.5})O_{19.5}$ secondary phase.

Surface morphology

Figure 2 presents the micro-structural images of $BiFeO_3$ and $BiFe_{0.95}Zn_{0.05}O_3$ sintered ceramics. The surface morphologies of both ceramics were dense with interconnected structure. It can be seen that with incorporation of 0.05 % Zn in $BiFeO_3$ results in agglomeration with uniform distribution of particles over the surface.

Ferroelectric P-E hysteresis loops

Figure 3 elucidates the P–E hystersis loops of $BiFeO_3$ and $BiFe_{0.95}Zn_{0.05}O_3$ ceramics sintered at 625°C and 650°C for 15 min. The ferroelectric (P–E) loops were measured at room temperature. The P–E loop shows unsaturated behavior due to lower resistivity of samples which results in higher leakage current and indicates a partial reversal of polarization. These leakage current values were observed because of increasing Zn doping in $BiFeO_3$ and charge neutralization of Zn^{2+} doping at Fe^{3+} site. Hence, it could be resulted into higher leakage

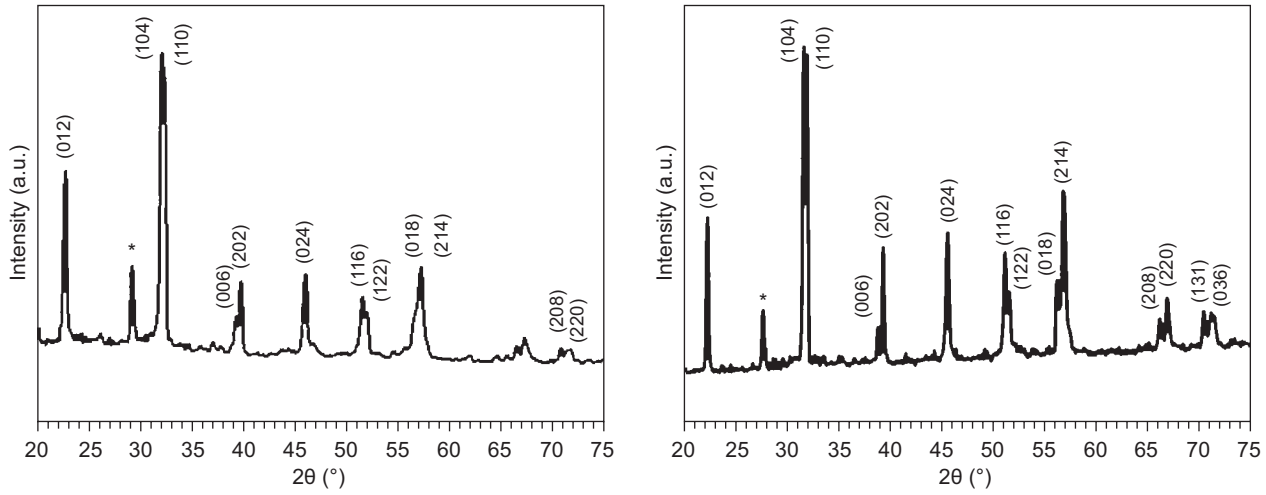

a) $BiFeO_3$ b) $BiFe_{0.95}Zn_{0.05}O_3$

Figure 1. X-ray diffraction (XRD) spectra of a) $BiFeO_3$ and b) $BiFe_{0.95}Zn_{0.05}O_3$ samples at room temperature.

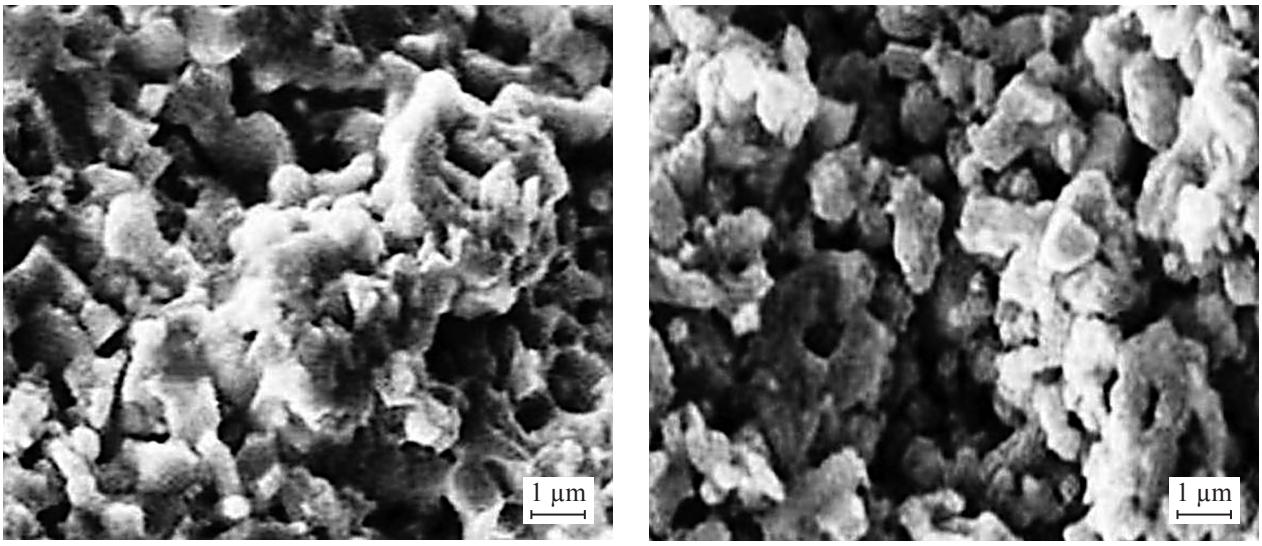

a) $BiFeO_3$ b) $BiFe_{0.95}Zn_{0.05}O_3$

Figure 2. Scanning electron micrographs (SEM) of (a) $BiFeO_3$ and (b) $BiFe_{0.95}Zn_{0.05}O_3$ samples.

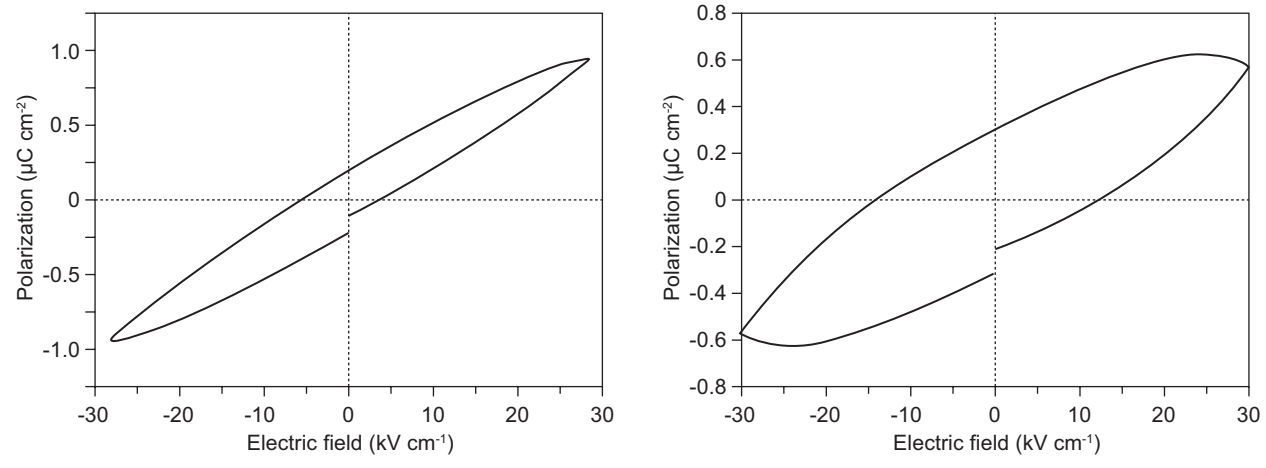

a) $BiFeO_3$ b) $BiFe_{0.95}Zn_{0.05}O_3$

Figure 3. Room temperature (RT) P–E hystersis loops for a) $BiFeO_3$, b) $BiFe_{0.95}Zn_{0.05}O_3$ ceramics.

current in $BiFeO_3$ and $BiFe_{0.95}Zn_{0.05}O_3$ compounds. The ionic radius of Zn^{2+} is slightly larger than that of Fe^{3+} hence deviation from original values of lattice parameters "a" and "c" is expected which will result in slight shifting of the diffraction peaks. Furthermore, the c/a ratio and Zn incorporation should not affects the crystalline structure of the parent compound $BiFeO_3$. This is crucial for enduring ferroelectric characteristics in $BiFeO_3$ and $BiFe_{0.95}Zn_{0.05}O_3$ ceramics.

Magnetic M-H hysteresis loops

Figure 4 presents the room temperature magnetic (M–H) hystersis loop of $BiFe_{0.95}Zn_{0.05}O_3$ ceramic. The M–H dependency of $BiFe_{0.95}Zn_{0.05}O_3$ ceramics has linear character upto 5 kOe, therefore confirming the weak ferromagnetic nature of $BiFe_{0.95}Zn_{0.05}O_3$ sample at 300 K. The room temperature low field M-H data upto 3 kOe for $BiFe_{0.95}Zn_{0.05}O_3$ ceramic is depicted in inset of Figure 4.

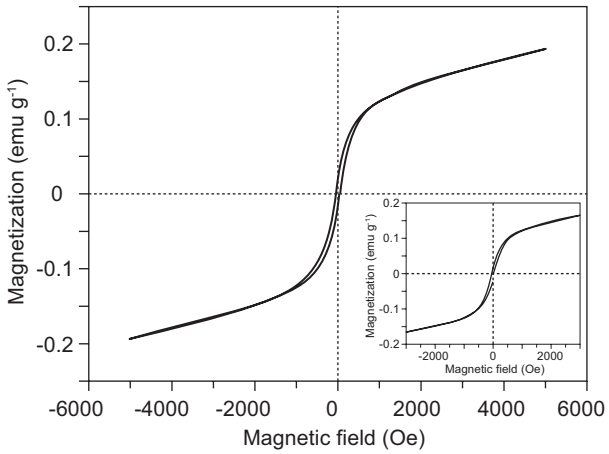

Figure 4. Room temperature M–H hystersis loops under the applied magnetic field of 5 kOe of $BiFe_{0.95}Zn_{0.05}O_3$ sample. (Inset shows low field M–H data at 3 kOe for the sample).

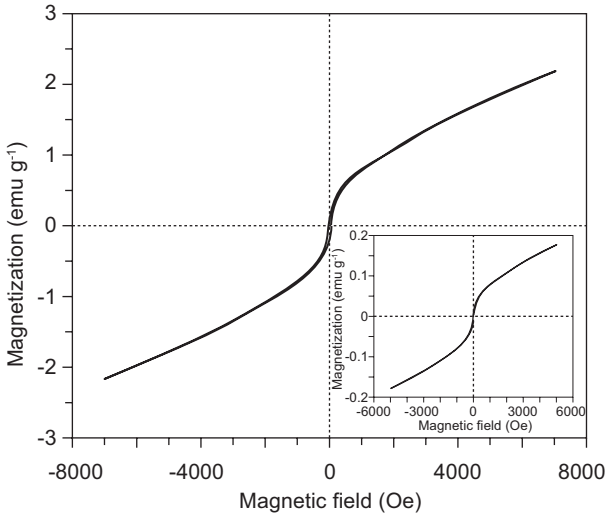

Figure 5. Magnetic hystersis loop at 5 K under the applied magnetic field of 70 kOe for $BiFe_{0.95}Zn_{0.05}O_3$/Inset shows low field M–H data at 50 kOe of $BiFe_{0.95}Zn_{0.05}O_3$ sample.

At 5 K, the magnetization measurement of $BiFe_{0.95}Zn_{0.05}O_3$ ceramic as a function of applied magnetic field shown in Figure 5. The low field M-H data upto 50 kOe for $BiFe_{0.95}Zn_{0.05}O_3$ ceramic at 5 K is depicted in inset of Figure 5. The values of coercive fields were found to be 79 and 355 Oe respectively at 300 and 5 K for $BiFe_{0.95}Zn_{0.05}O_3$ ceramics.

The temperature dependence magnetization measurement of $BiFe_{0.95}Zn_{0.05}O_3$ ceramic at 5 K with applied field of 5 kOe shown in Figure 6. With increasing temperature the magnetization decreases for $BiFe_{0.95}Zn_{0.05}O_3$ sample.

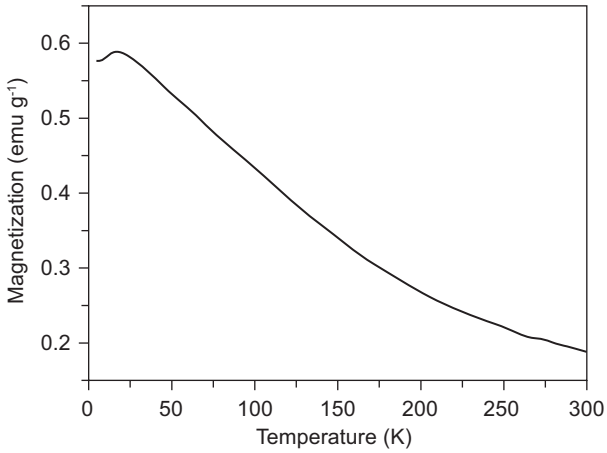

Figure 6. M–T curve under magnetic field of 5000 Oe for $BiFe_{0.95}Zn_{0.05}O_3$ ceramic sample.

Dielectric measurements

Figure 7 depicts the temperature dependence of dielectric constant for $BiFeO_3$ and $BiFe_{0.95}Zn_{0.05}O_3$ ceramics. The frequency was varied from 1 - 5 kHz. The dielectric constant delivers a continuous increase with temperature for both $BiFeO_3$ and $BiFe_{0.95}Zn_{0.05}O_3$ ceramics. In our case, a clear dielectric anomaly has been addressed in $BiFeO_3$ and $BiFe_{0.95}Zn_{0.05}O_3$ ceramics approximately around 480°C and 450°C. This anomaly seems to be correlated with phase transformation from antiferromagnetic to paramagnetic phase and also manifests a possible coupling between electric and magnetic dipole moments in $BiFeO_3$ [25, 26]. The room temperature measured values of dielectric constant for $BiFeO_3$ and $BiFe_{0.95}Zn_{0.05}O_3$ ceramics were found to be 34 and 44 respectively at 1 kHz.

CONCLUSIONS

We have synthesized the $BiFeO_3$ and $BiFe_{0.95}Zn_{0.05}O_3$ bulk multiferroic ceramics by self propagating high temperature synthesis (SHS). The room temperature

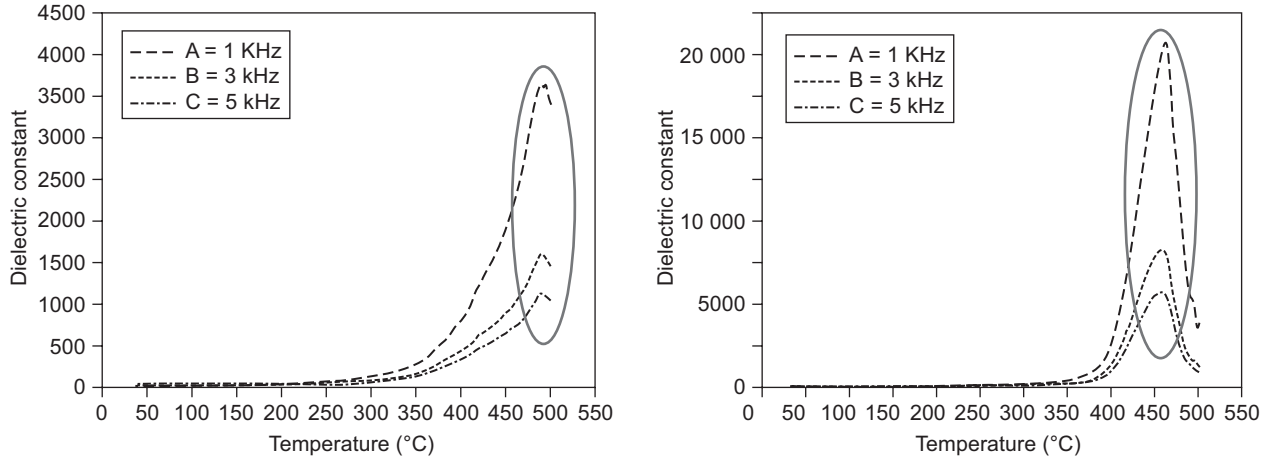

a) $BiFeO_3$ b) $BiFe_{0.95}Zn_{0.05}O_3$

Figure 7. Dielectric constant versus temperature measurements in the frequency range 1- 5 kHz for a) $BiFeO_3$ (curve A-C) and b) $BiFe_{0.95}Zn_{0.05}O_3$ (curve A-C).

ferroelectric and magnetic hystersis loop attests the co-existence of ferroelectricity and magnetism. Magnetization measurement of $BiFe_{0.95}Zn_{0.05}O_3$ samples at 300 K and 5 K demonstrates a weak ferromagnetism. The P–E hystersis loops of $BiFeO_3$ and $BiFe_{0.95}Zn_{0.05}O_3$ ceramics represents an unsaturated behavior and indicates partial reversal of polarization. A dielectric measurement of $BiFeO_3$ ceramic exhibits an apparent dielectric anomaly around 480°C and 450°C which proves an antiferromagnetic to paramagnetic phase transition (T_N) of $BiFeO_3$.

Acknowledgements

The authors are greatful to UGC-SAP-DRS Phase II (India) for support.

REFERENCES

1. Cheong S.W., Mostovoy M.: Nature Mater. *6*, 13 (2007).
2. Kumar N., Panwar N., Gahtori B., Singh N., Kishan H., Awana V.P.S: J. Alloy. Comp. *501*, 129 (2010).
3. Khomchenko V.A., Kiselev D.A., Kopcewicz M., Maglione M., Shvartsman V.V., Borisov P., Kleeman W., Lopes A.M.L, Pogorelev Y.G., Araujo J.P., Rubinger R.B., Sobolev N.A., Vieira J.M., Kholkin A.L.: J. Magn. Magn. Mater. *321*, 1692 (2009).
4. Spaldin N.A., Fiebig M.: Science *309*, 391 (2005).
5. Kumar M., Yadav K.L.: Appl. Phys. Lett. *91*, 242901 (2007).
6. Garcia F.G., Riccardi C.S., Simoes A.Z.: J. Alloy. Comp. *501*, 25 (2010).
7. Varshney D., Kumar A., Verma K.: J. Alloy. Comp. *509*, 8421 (2011).
8. Wang Y., J. Alloy. Comp. *509*, 1362 (2011).
9. Shami M.Y., Awan M.S., Anis-ur-Rehman M.: J. Alloy. Comp. *509*, 10139 (2011).
10. Azam A., Jawad A., Ahmed A.S., Chaman M., Naqvi A. H.: J. Alloy. Comp. *509*, 2909 (2011).
11. Mazumder R., Sen A.: J. Alloy. Comp. *475*, 577 (2009).
12. Azough F., Freer R., Thrall M., Cernik R., Tuna F., Collison D.: J. Eur. Ceram. Soc. *30*, 727 (2010).
13. Mathe V.L., Patankar K.K., Patil R.N., Lokhande C.D.: J. Magn. Magn. Mater. *270*, 380 (2004).
14. Jiang Q.H., Nan C.W., Shen Z.J.: J. Amer. Ceram. Soc. *89*, 21 (2006).
15. Kim D.H., Lee H.N., Biegalski M.D., Christen H.M.: Appl. Phys. Lett. *91*, 042906 (2007).
16. Kumar M., Yadav K.L.: J. Appl. Phys. *100*, 074111 (2006).
17. Nalwa K.S., Garg A., Upadhyaya A.: Mater. Lett. *62*, 878 (2008).
18. Kothari D., Reddy V.R., Gupta A., Sathe V., Banerjee A., Gupta S.M., Awasthi A.M.: Appl. Phys. Lett. *88*, 212907 (2006).
19. Wang D.H., Goh W.C., Ning M., Ong C.K.: Appl. Phys. Lett. *88*, 212907 (2006).
20. Gautam A., Rangra V.S.: Cryst. Res. Tech. *45*, 953 (2010).
21. Xu Q., Zai H., Wu D., Tang Y.K., Xu M.X.: J. Alloy. Comp. *485*, 13 (2009).
22. Saha S., Ghanawat S.J., Purohit R.D.: J. Mater. Sci. *41*, 1939 (2006).
23. Chaudhari Y. A., Mahajan C. M., Jagtap P. P., Bendre S. T.: Journal of Advanced Ceramics *2*, 135 (2013).
24. Chaudhari Y. A., Mahajan C. M., Abuassaj E. M., Jagtap P. P., Patil P. B., Bendre S. T.: Materials Science-Poland *31*, 221 (2013).
25. Jia D.C., Xu J.H., Ke H., Wang W., Zhou Y.: J. Eur. Ceram. Soc. *29*, 3099 (2009).
26. Chaudhari Y. A., Singh A., Mahajan C. M., Jagtap P. P., Abuassaj E. M, Chatterjee R., Bendre S. T.: Journal of Magnetism and Magnetic Materials *347*, 153 (2013).